

# Universality of the Diffusion Wake from Stopped and Punch-Through Jets in Heavy-Ion Collisions

Barbara Betz,<sup>1</sup> Jorge Noronha,<sup>2</sup> Giorgio Torrieri,<sup>3</sup> Miklos Gyulassy,<sup>2,3</sup> Igor Mishustin,<sup>3</sup> and Dirk H. Rischke<sup>1,3</sup>

<sup>1</sup>*Institut für Theoretische Physik, Johann Wolfgang Goethe-Universität, Frankfurt am Main, Germany*

<sup>2</sup>*Department of Physics, Columbia University, New York, 10027, USA*

<sup>3</sup>*Frankfurt Institute for Advanced Studies (FIAS), Frankfurt am Main, Germany*

We solve (3+1)-dimensional ideal hydrodynamical equations with source terms that describe punch-through and fully stopped jets in order to compare their final away-side angular correlations in a static medium. For fully stopped jets, the backreaction of the medium is described by a simple Bethe-Bloch-like model which leads to an explosive burst of energy and momentum (Bragg peak) close to the end of the jet's evolution through the medium. Surprisingly enough, we find that the medium's response and the corresponding away-side angular correlations are largely insensitive to whether the jet punches through or stops inside the medium. This result is also independent of whether momentum deposition is longitudinal (as generally occurs in pQCD energy loss models) or transverse (as the Bethe-Bloch formula implies). The existence of the diffusion wake is therefore shown to be universal to all scenarios where momentum as well as energy is deposited into the medium, which can readily be understood in ideal hydrodynamics through vorticity conservation. The particle yield coming from the strong forward moving diffusion wake that is formed in the wake of both punch-through and stopped jets largely overwhelms their weak Mach cone signal after freeze-out.

PACS numbers: 13.90.+i, 25.75.Bh, 25.75.Gz

## I. INTRODUCTION

One of the major discoveries found at the Relativistic Heavy Ion Collider (RHIC) was the suppression of highly energetic particles in central A+A collisions [1, 2]. Jets are assumed to be created in the early stage of a heavy-ion collision where they interact with the hot and dense nuclear matter and serve as a hard probe for the created medium [3, 4, 5, 6, 7, 8, 9, 10, 11, 12]. Two- and three-particle correlations of intermediate- $p_{\perp}$  particles provide an important test of the medium response to the details of the jet quenching dynamics and they show a re-appearance of a broad or double-peaked structure in the away-side of jet angular correlations [13, 14, 15, 16, 17, 18].

The observation of strong elliptic flow in non-central Au+Au collisions consistent with fluid dynamical predictions [19, 20] suggests that a thermalized medium that evolves hydrodynamically is created in these collisions. Moreover, since the average momentum of particles emitted on the away-side approaches the value of the thermalized medium with decreasing impact parameter [15], the energy lost by the jet should quickly thermalize. Thus, the disturbance caused by the jet may also be described hydrodynamically.

Recent interest in Mach-like conical di-jet correlations is based on suggestions [21, 22, 23, 24, 25, 26] that a measurement of the dependence on the cone angle associated with a supersonic jet moving with velocity  $v$  could provide via Mach's law ( $\cos \phi_M = c_s/v$ ) a constraint on the average speed of sound in the strongly coupled Quark-Gluon Plasma (sQGP) [27, 28]. For a quantitative comparison to RHIC data, a detailed model of both energy and momentum deposition coupled to a relativistic fluid

model is needed [23, 26, 29, 30, 31, 32, 33, 34, 35].

In general, supersonic probes that shoot through a fluid can deposit energy and momentum in the medium in such a way that collective excitations such as Mach cones and diffusion wakes are formed [36]. These structures have indeed been found [37, 38] in the wake of a supersonic heavy quark that travels through an  $\mathcal{N} = 4$  Supersymmetric Yang-Mills (SYM) thermal plasma [39, 40, 41]. The validity of a hydrodynamic description of the supersonic heavy quark wake was studied in Refs. [42, 43, 44, 45, 46] in the framework of the Anti-de Sitter/Conformal Field Theory correspondence (AdS/CFT) [47, 48]. The angular correlations created by heavy quark jets in AdS/CFT have recently been computed in Ref. [49, 50, 51] and compared [52] to the results obtained by a punch-through heavy quark jet described by the Neufeld *et. al.* [53, 54, 55] chromo-viscous hydrodynamic model, which is formulated within perturbative quantum chromodynamics (pQCD).

In general, a fast moving parton (which could be a light quark/gluon or a heavy quark) will lose a certain amount of its energy and momentum along its path through the medium and then decelerate. Thus, the fate of the parton jet strongly depends on its initial energy: if the parton has enough energy it can punch through the medium and fragment in the vacuum (punch-through jet) or it can be severely quenched until it becomes part of the thermal bath (stopped jet). Of course, the amount of initial energy required for the parton to punch through depends on the properties of the medium (a very large energy loss per unit length  $dE/dx$  means that most of the jets will be quenched while only a few would have enough energy to leave the plasma). In this paper we solve the (3+1)-dimensional ideal hydrodynamical equations [56]

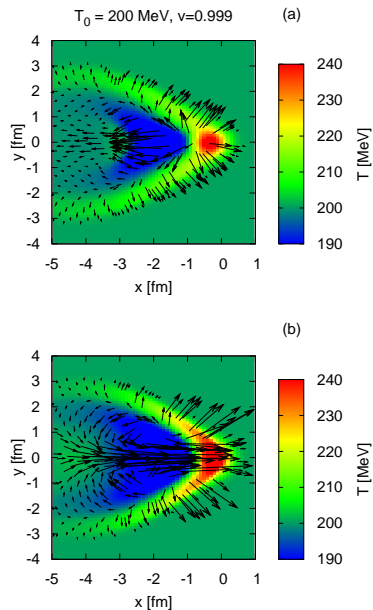


FIG. 1: (Color online) Temperature pattern and flow velocity profile (arrows) after a hydrodynamical evolution of  $t = 4.5/v_{\text{jet}}$  fm, assuming (a) an energy loss rate of  $dE/dt = 1.5$  GeV/fm for a vanishing momentum loss rate and (b) an energy and momentum loss rate of  $dE/dt = dM/dt = 1.5$  GeV/fm for a punch-through jet moving with a constant velocity of  $v_{\text{jet}} = 0.999$  along the  $x$ -axis through a static background plasma with temperature  $T_0 = 200$  MeV. The jet is sitting at the origin of the coordinates at the time of freeze-out.

with source terms that describe the two scenarios in order to compare the final away-side angular correlations produced by a punch-through and a fully stopped jet in a static medium with background temperature  $T_0$ . We would like to point out that the wake formed by fully stopped jets has not yet been studied using hydrodynamics.

For simplicity, our medium is a gas of massless  $SU(3)$  gluons in which  $p = e/3$ , where  $p$  and  $e$  are the pressure and the energy density, respectively. An isochronous Cooper–Frye (CF) [57] freeze-out procedure is employed in order to obtain the angular distribution of particles associated with the away-side jet. We use a simplified Bethe–Bloch model [58] to show that the explosive burst of energy and momentum [known as the Bragg peak [59, 60, 61, 62]] deposited by a fully quenched jet immediately before it thermalizes does not stop the diffusion wake and, thus, no new structures in the away-side of angular correlation functions can be found. This explosive release of energy before complete stopping is a general phenomenon that has been employed, for instance, in applications of particle beams for cancer therapy [63, 64, 65].

This paper is organized as follows. In Sec. II we

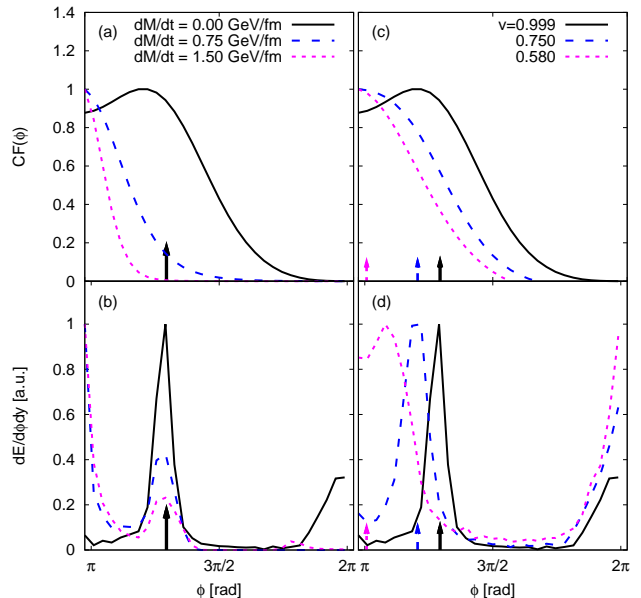


FIG. 2: (Color online) The left panels show the normalized angular distribution created by a punch-through jet at mid-rapidity with a fixed energy loss of  $dE/dt = 1.5$  GeV/fm and different momentum loss rates. The jet moves at a constant velocity  $v_{\text{jet}} = 0.999$  through the medium. The right panels show the angular distributions associated with jets where  $dE/dt = 1.5$  GeV/fm and vanishing momentum loss ( $dM/dt = 0$ ). Here, the jets move with different velocities through the medium:  $v_{\text{jet}} = 0.999$  (black),  $v_{\text{jet}} = 0.75$  (blue), and  $v_{\text{jet}} = 0.58$  (magenta). In the upper panels, an isochronous Cooper–Frye freeze-out at  $p_{\perp} = 5$  GeV is used while in the lower panels we employed the bulk flow freeze-out procedure [52]. The arrows indicate the angle of the Mach cone as computed via Mach’s law.

describe how a jet deposits energy and momentum in (3+1)-dimensional hydrodynamics and how we extract observables for the Mach cone created by the away-side jet. In Sec. III we present our results for punch-through, and in Sec. IV for completely stopped jets. A summary concludes this paper in Sec. V.

We use natural units and the Minkowski metric  $g_{\mu\nu} = \text{diag}(+, -, -, -)$ . Lorentz indices are denoted with Greek letters  $\mu, \nu = 0, \dots, 3$ . In our system of coordinates, the beam axis is aligned with the  $z$ -direction and the associated jet moves along the  $x$ -direction with velocity  $\vec{v} = v \hat{x}$ .

## II. JETS IN IDEAL HYDRODYNAMICS

Energetic back-to-back jets produced in the early stages of a heavy-ion collision transverse to the beam axis can travel through the sQGP and deposit energy and momentum along their path in a way that depends

on the physics behind the interaction between the jet and the underlying medium. In the case where one of the jets is produced near the surface (trigger jet), the other supersonic away-side jet moves through the medium and excites a Mach wave as well as a diffusion wake. The resulting angular correlation with respect to the away-side jet axis is then expected to lead to an enhancement of associated hadrons at the characteristic Mach angle [23, 24, 25, 26, 30].

In ideal hydrodynamics, the energy–momentum tensor

$$T^{\mu\nu} = (e + p)u^\mu u^\nu - pg^{\mu\nu}, \quad (1)$$

is locally conserved, i.e.,

$$\partial_\mu T^{\mu\nu} = 0, \quad (2)$$

where  $u^\mu = \gamma(1, \vec{v})$  is the flow 4-velocity and  $\gamma = (1 - \vec{v}^2)^{-1/2}$ . We take the net baryon density to be identically zero in this study. Here, we only consider a static medium. More realistic initial conditions involving an expanding medium will be considered in a further study.

Once the jet is included in the system the conservation equations change. We assume that the energy lost by the jet thermalizes and gives rise to a source term  $S^\nu$  in the energy–momentum conservation equations

$$\partial_\mu T^{\mu\nu} = S^\nu. \quad (3)$$

Thus, one has to solve Eq. (3) numerically in order to determine the time evolution of the medium which was disturbed by the moving jet. The source term that correctly depicts the interaction of the jet with the sQGP is unknown from first principles, although recent calculations in AdS/CFT [42, 43, 44] and pQCD [54] have shed some light on this problem. While pQCD is certainly the correct description in the hard-momentum region where jets are produced ( $Q \gg T_0$ ), in the soft part of the process ( $Q \sim T_0$ ) non-perturbative effects may become relevant.

In this paper, we omit the near-side correlations associated with the trigger jet and assume that the away-side jet travels through the medium according to a source term that depends on the jet velocity profile which shall be discussed below for the case of punch-through and stopped jets.

The away-side jet is implemented in the beginning of the hydrodynamical evolution at  $x = -4.5$  fm, and its motion is followed until it reaches  $x = 0$ . For a jet moving with a constant velocity  $v_{\text{jet}}$  this happens at  $t_f = 4.5/v_{\text{jet}}$  fm.

We use two different methods to obtain the away-side angular correlations. In the CF method [57], the fluid velocity  $u^\mu(t_f, \vec{x})$  and temperature  $T(t_f, \vec{x})$  fields are converted into free particles at a freeze-out surface  $\Sigma$  at constant time  $t_f$ . In principle, one has to ensure that energy and momentum are conserved during the freeze-out procedure [66]. However, the associated corrections are zero if the equation of state is the same before and after the freeze-out, as it is assumed in the present study. In this

case, the momentum distribution for associated (massless) particles  $p^\mu = (p_\perp, p_\perp \cos(\pi - \phi), p_\perp \sin(\pi - \phi))$  at mid-rapidity  $y = 0$  is computed via

$$\frac{dN_{\text{ass}}}{p_\perp dp_\perp dy d\phi} \Big|_{y=0} = \int_\Sigma d\Sigma_\mu p^\mu [f_0(u^\mu, p^\mu, T) - f_{\text{eq}}]. \quad (4)$$

Here,  $\phi$  is the azimuthal angle between the emitted particle and the trigger,  $p_\perp$  is the transverse momentum,  $f_0 = \exp[-u^\mu(t, \vec{x})p_\mu/T(t, \vec{x})]$  the local Boltzmann equilibrium distribution, and  $f_{\text{eq}} \equiv f|_{u^\mu=0, T=T_0}$  denotes the isotropic background yield. We checked that our results do not change significantly if we use a Bose–Einstein distribution instead of the Boltzmann distribution. The background temperature is set to  $T_0 = 0.2$  GeV. Following Refs. [23, 26, 33, 50], we perform an isochronous freeze-out where  $d\Sigma^\mu = d^3\vec{x}(1, 0, 0, 0)$  and define the angular function

$$CF(\phi) = \frac{1}{N_{\text{max}}} \frac{dN_{\text{ass}}(\phi)}{p_\perp dp_\perp dy d\phi} \Big|_{y=0}, \quad (5)$$

where the constant  $N_{\text{max}}$  is used to normalize the plots. We would like to remark that in the associated  $p_\perp$ –range of interest a coalescence/recombination hadronization scenario [67, 68, 69, 70, 71] may be more appropriate than CF freeze-out. However, we expect that the main features of the away-side angular correlations obtained using CF hadronization are robust enough to survive other hadronization schemes.

The other freeze-out prescription (called bulk flow freeze-out) used in the present paper was introduced in Ref. [52]. The main assumption behind the bulk flow freeze-out is that all the particles inside a given small sub-volume of the fluid will be emitted in the same direction as the average local energy flow

$$\frac{d\mathcal{E}}{d\phi dy} = \int d^3\vec{x} \mathcal{E}(\vec{x}) \delta[\phi - \Phi(\vec{x})] \delta[y - Y(\vec{x})]. \quad (6)$$

Here,  $\phi$  is again the azimuthal angle between the detected particle and the trigger jet and  $y$  is the particle rapidity. Only the  $y = 0$  yield is considered. The cells are selected according to their local azimuthal angle  $\Phi(\vec{x}) = \arctan[\mathcal{P}_y(\vec{x})/\mathcal{P}_x(\vec{x})]$  and rapidity  $Y(\vec{x}) = \text{Arctanh}[\mathcal{P}_z(\vec{x})/\mathcal{E}(\vec{x})]$ . The local momentum density of the cell is  $T^{0i}(\vec{x}) = \mathcal{P}_i(\vec{x})$ , while its local energy density in the lab frame is  $\mathcal{E}(\vec{x}) = T^{00}(\vec{x})$ . The  $\delta$ -functions are implemented using a Gaussian representation as in Ref. [52]. Due to energy and momentum conservation, this quantity should be conserved after freeze-out. Note that Eq. (6) is not restricted to a certain  $p_\perp$  and does not include the thermal smearing that is always present in the CF freeze-out.

### III. PUNCH-THROUGH JETS

In this section we consider a jet moving with a uniform velocity  $v_{\text{jet}} = 0.999$  through the medium. The source

term is given by

$$S^\nu = \int_{\tau_i}^{\tau_f} d\tau \frac{dM^\nu}{d\tau} \delta^{(4)} \left[ x^\mu - x_{\text{jet}}^\mu(\tau) \right], \quad (7)$$

where  $\tau_f - \tau_i$  denotes the proper time interval associated with the jet evolution. We further assume a constant energy and momentum loss rate  $dM^\nu/d\tau = (dE/d\tau, d\vec{M}/d\tau)$  along the trajectory of the jet  $x_{\text{jet}}^\mu(\tau) = x_0^\mu + u_{\text{jet}}^\mu \tau$ . In non-covariant notation, this source term has the form

$$S^\nu(t, \vec{x}) = \frac{1}{(\sqrt{2\pi}\sigma)^3} \exp \left\{ -\frac{[\vec{x} - \vec{x}_{\text{jet}}(t)]^2}{2\sigma^2} \right\} \times \left( \frac{dE}{dt}, \frac{dM}{dt}, 0, 0 \right), \quad (8)$$

where  $\vec{x}_{\text{jet}}$  describes the location of the jet,  $\vec{x}$  is the position on the computational grid, and  $\sigma = 0.3$ . The system plasma+jet evolves according to Eq. (3) until the freeze-out time  $t_f = 4.5/v_{\text{jet}}$  fm is reached.

The temperature and flow velocity profiles created by a punch-through jet with a constant energy loss rate of  $dE/dt = 1.5$  GeV/fm and vanishing momentum deposition are shown in Fig. 1 (a). In Fig. 1 (b) the jet has lost the same amount of energy and momentum and in this case one can clearly see that the space-time region close to the jet, where the temperature disturbance is the largest, is bigger than in the pure energy deposition scenario. The creation of a diffusion wake behind the jet in the case of equal energy and momentum deposition is clearly visible, which is indicated by the strong flow observed in the forward direction (at  $\phi = \pi$ ).

Note in Fig. 2 (a) that for the punch-through jet deposition scenario with equal energy and momentum loss one always obtains a peak in the associated jet direction after performing the freeze-out using the two prescriptions described in Sec. II. However, the energy flow distribution in Fig. 2 (b) displays an additional small peak at the Mach cone angle indicated by the arrow. This Mach signal cannot be seen in the Cooper–Frye freeze-out because of thermal smearing [23, 33, 50, 52] and the strong influence of the diffusion wake, which leads to the strong peak around  $\phi \sim \pi$  in the bulk energy flow distribution.

However, given that the exact form of the source term in the sQGP is unknown, one may want to explore other energy–momentum deposition scenarios where the jet deposits more energy than momentum along its path. While this may seem unlikely, such a situation cannot be ruled out. Thus, for the sake of completeness, we additionally consider in Fig. 2 (a) the case where the jet source term is described by a fixed energy loss of  $dE/dt = 1.5$  GeV/fm and different momentum loss rates. In the bulk flow distribution in Fig. 2 (b), one can see that the peak at the Mach cone angle is more pronounced for smaller momentum loss while the contribution of the diffusion wake (indicated by the peak in forward direction)

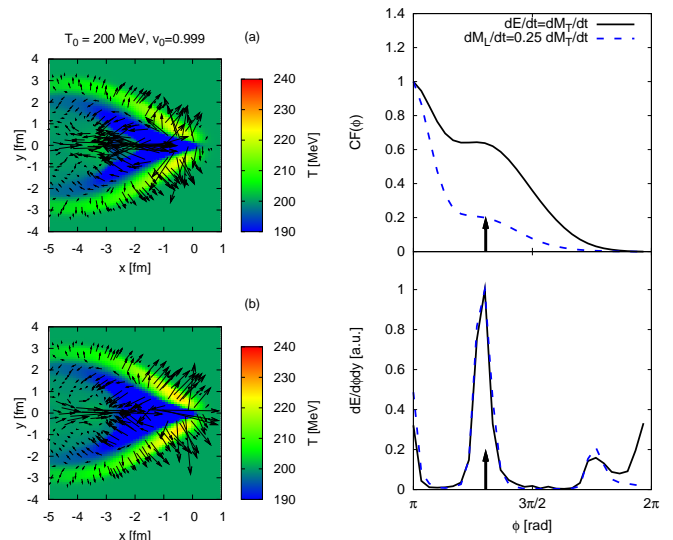


FIG. 3: (Color online) Left panel: Temperature pattern and flow velocity profile (arrows) after a hydrodynamical evolution of  $t = 4.5/v_{\text{jet}}$  fm, assuming an energy loss rate of  $dE/dt = dM/dt = 1.5$  GeV/fm for (a) full transverse momentum deposition and (b) longitudinal as well as transverse momentum deposition with a ratio of  $dM_L/dt = 0.25 dM_T/dt$ . Right panel: The normalized angular distribution created by a punch-through jet at mid-rapidity for the two above mentioned transverse momentum deposition scenarios. In the upper panel, an isochronous Cooper–Frye freeze-out at  $p_\perp = 5$  GeV is used while in the lower panel the bulk flow freeze-out procedure [52] is employed. The arrows indicate the ideal Mach cone angle.

is reduced. The associated particle distribution from the CF freeze-out in Fig. 2 (a) reveals a peak at  $\phi \neq \pi$  for pure energy deposition (solid black line), however, the opening angle is shifted to a value smaller than the Mach cone angle due to thermal smearing [33].

In Figs. 2 (c,d) we consider  $dM/dt = 0$  jets that move through the medium with different velocities  $v_{\text{jet}} = 0.999, 0.75$ , and  $0.58$ . Note in Fig. 2 (d) that the peak position changes in the bulk flow distribution according to the expected Mach cone angles (indicated by the arrows). However, due to the strong bow shock created by a jet moving at a slightly supersonic velocity of  $v_{\text{jet}} = 0.58$ , there is a strong contribution in the forward direction in this case and the peak position is shifted from the expected value. In the CF freeze-out shown in Fig. 2 (c), the peak from the Mach cone can again be seen for the jet moving nearly at the speed of light ( $v_{\text{jet}} = 0.999$ ), but for slower jets thermal smearing again leads to a broad distribution peaked in the direction of the associated jet.

It is apparently surprising that the above mentioned results are independent of whether the momentum deposited by the particle is in the longitudinal (along the motion of the jet) or transversal (perpendicular) direc-

tion. Repeating the calculation shown in Fig. 1 including transverse momentum deposition

$$S^\nu(t, \vec{x}) \propto \begin{bmatrix} dE/dt \\ dM_L/dt \\ (dM_T/dt) \cos \varphi \\ (dM_T/dt) \sin \varphi \end{bmatrix}, \quad (9)$$

where  $\varphi$  is the latitude angle in the  $y - z$  plane with respect to the jet motion and the magnitude of  $S^\nu(t, \vec{x})$  is the same as Eq. (7), shows that transverse momentum deposition will not alter the results presented in this section (see Fig. 3). A longitudinal diffusion wake still forms during the fluid evolution stage, and its contribution will still dominate the resulting angular inter-particle correlations though a peak occurs around the expected Mach cone angle in the CF freeze-out.

The reason is that transverse momentum deposition will force the fluid around the jet to expand, and the empty space left will create a shock wave in the longitudinal direction that behaves much like a diffusion wake. In terms of ideal hydrodynamics, this universality of the diffusion wake can be understood in the context of vorticity conservation since momentum deposition, whether transverse or longitudinal, will add vorticity to the system. This vorticity will always end up behaving as a diffusion wake [72]. In the next section, we demonstrate that these results are largely independent of whether the jet is fully quenched or survives as a hard trigger.

#### IV. STOPPED JETS

In the previous section we considered a uniformly moving jet that deposited energy and/or momentum in the medium at a constant rate. However, due to its interaction with the plasma, the jet will decelerate and its energy and/or momentum loss will change. Thus, the deceleration roughly represents the response of the medium. In general, a decelerating jet should have a peak in the energy loss rate because the interaction cross section increases as the parton's energy decreases. In other words, when the particle's velocity goes to zero there appears a peak in  $dE/dx$  known as the Bragg peak [59]. The question to be considered in this section is whether this energy deposition scenario might be able to somehow stop the diffusion wake and, thus, change the angular distributions shown in Fig. 2. The source term in this case is still given by Eq. (8) and, according to the Bethe–Bloch formalism [59, 60, 61, 62], one assumes that

$$\frac{dE(t)}{dt} = a \frac{1}{v_{\text{jet}}(t)}, \quad (10)$$

which shows that when the jet decelerates the energy loss rate increases and has a peak as  $v_{\text{jet}} \rightarrow 0$ . Note that here  $dE/dt$  is the energy lost by the jet, which is the negative of the energy given to the plasma. Using this ansatz for the velocity dependence of the energy loss rate

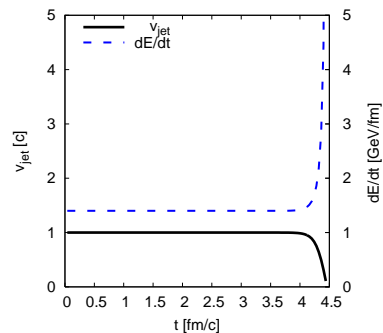


FIG. 4: (Color online) The jet velocity  $v_{\text{jet}}(t)$  (solid black line) and energy deposition rate  $dE(t)/dt$  (dashed blue line) according to Eq. (12). The initial jet velocity and energy loss rate are  $v_{\text{jet}} = 0.999$  and  $a \simeq -1.3607$  GeV/fm, respectively.

and the identities  $dE/dt = v_{\text{jet}} dM/dt$  and  $dM/dy_{\text{jet}} = m \cosh y_{\text{jet}}$  (as well as  $v_{\text{jet}} = \tanh y_{\text{jet}}$ ), one can rewrite Eq. (10) as

$$t(y_{\text{jet}}) = \frac{m}{a} \left[ \sinh y_{\text{jet}} - \sinh y_0 - \arccos \frac{1}{\cosh y_{\text{jet}}} + \arccos \frac{1}{\cosh y_0} \right], \quad (11)$$

where  $y_0$  is the jet's initial rapidity. The equation above can be used to determine the time-dependent velocity  $v_{\text{jet}}(t)$ . The initial velocity is taken to be  $v_0 = \text{Artanh} y_0 = 0.999$ . The mass of the moving parton is taken to be of the order of the constituent quark mass  $m = 0.3$  GeV. Moreover, the initial energy loss rate  $a \simeq -1.3607$  GeV/fm is determined by imposing that the jet stops after  $\Delta x = 4.5$  fm (as in the previous section for a jet with  $v_{\text{jet}} = 0.999$ ). Thus, the jet location as well as the energy and momentum deposition can be calculated as a function of time via the following equations

$$x_{\text{jet}}(t) = x_{\text{jet}}(0) + \frac{m}{a} [(2 - v_{\text{jet}}^2) \gamma_{\text{jet}} - (2 - v_0^2) \gamma_0], \quad (12)$$

$$\frac{dE}{dt} = a \frac{1}{v_{\text{jet}}}, \quad \frac{dM}{dt} = a \frac{1}{v_{\text{jet}}^2},$$

which can be used to determine the corresponding source term for the energy-momentum conservation equations. The change of the jet velocity  $v_{\text{jet}}(t)$  and energy deposition  $dE(t)/dt$  are displayed in Fig. 4. The strong increase of energy deposition shortly before the jet is completely stopped corresponds to the well-known Bragg peak [59].

The main difference between the ansatz described here and the Bethe–Bloch equation is that the momentum deposition is longitudinal (parallel to the motion of the jet) rather than transverse (perpendicular to the motion of the jet). According to most pQCD calculations, this is true in the limit of an infinite energy jet [3, 4, 5, 6, 7, 8, 9, 10, 11, 12], but it is expected to break down in the vicinity of the Bragg peak where the jet energy is comparable to the energy of a thermal particle. However, as we demonstrated in the previous section, the

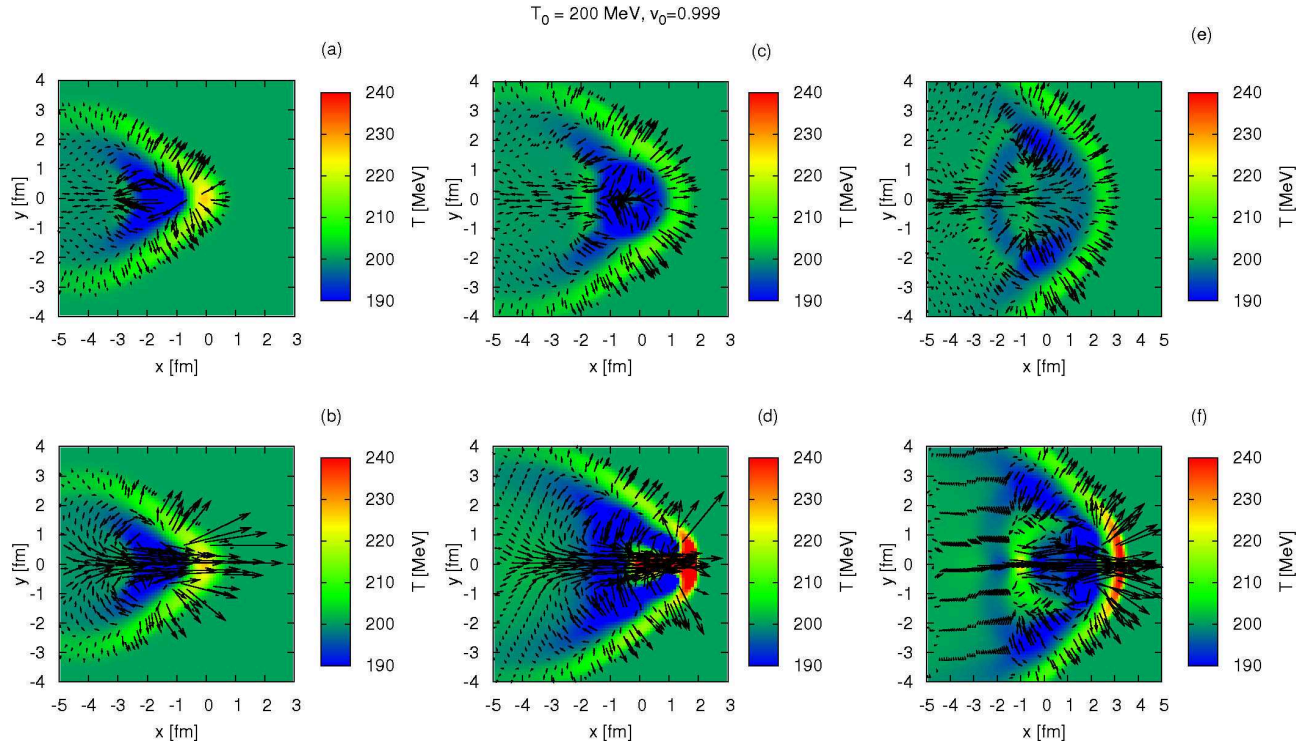


FIG. 5: (Color online) Temperature pattern and flow velocity profile (arrows) after a hydrodynamical evolution of  $t = 4.5$  fm (left panel),  $t = 6.5$  fm (middle panel) and  $t = 8.5$  fm (right panel) for a jet that decelerates according to the Bethe–Bloch formula and stops after  $\Delta x = 4.5$  fm. The jet’s initial velocity is  $v_{\text{jet}} = 0.999$ . In the upper panel a vanishing momentum loss rate is assumed while in the lower panel the momentum loss is related to the energy loss by Eq. (12).

freeze-out phenomenology is rather insensitive to whether the momentum deposition is transverse or longitudinal.

Fig. 5 displays the temperature and flow velocity profiles of a jet that stops after  $\Delta x = 4.5$  fm, with an energy loss according to Eq. (10) and vanishing momentum deposition (upper panel) as well as an energy and momentum deposition following Eq. (12) (lower panel). In the left panel the medium decouples immediately after  $t = 4.5$  fm when the jet is stopped while in the middle and right panel the decoupling takes place after  $t = 6.5$  fm and  $t = 8.5$  fm, respectively.

Comparing this result to Fig. 1 leads to the conclusion that the diffusion wake is present independent of whether the jet is quenched or survives until freeze-out. In the former case, however, the diffusion wake is only weakly sensitive to the duration of the subsequent evolution of the system.

Within ideal hydrodynamics this can be understood via vorticity conservation. The vorticity-dominated diffusion wake will always be there in the ideal fluid, whether the source of vorticity has been quenched or not. The only way this vorticity can disappear is via viscous dissipation. While a (3+1)–dimensional viscous hydrodynamic calculation is needed to quantify the effects of this dissipation, linearized hydrodynamics predicts that

both Mach cones and diffusion wakes are similarly affected [23, 26, 36].

The angular distribution associated with the decelerating jet (which stops after  $\Delta x = 4.5$  fm), shown in Fig. 6, is determined according to the two freeze-out prescriptions described in Sec. II. When the energy and momentum loss rates are determined by Eq. (12) (magenta line), both freeze-out procedures display a feature discussed in the previous section for the case of punch-through jets: the formation of a strong diffusion wake which leads to a strong peak in the associated jet direction. The results after the isochronous CF freeze-out are shown in the upper panel of Fig. 6. As in Fig. 5, the medium decouples after  $t = 4.5$  fm (left panel),  $t = 6.5$  fm (middle panel) and  $t = 8.5$  fm (right panel). Only the pure energy deposition scenario produces a peak at an angle close to the Mach angle [see Fig. 6 (a)] which is smeared out thermally for larger decoupling times [cf. Fig. 6 (b) and (c)]. On the other hand, the bulk energy flow freeze-out displayed (lower panel) shows in all cases a peak at the Mach cone angle. Note that in this case the peak becomes more pronounced when  $dM/dt = 0$ . While the Mach cone signal increases with the decay time, the signal is still smaller than the forward yield of the diffusion wake.

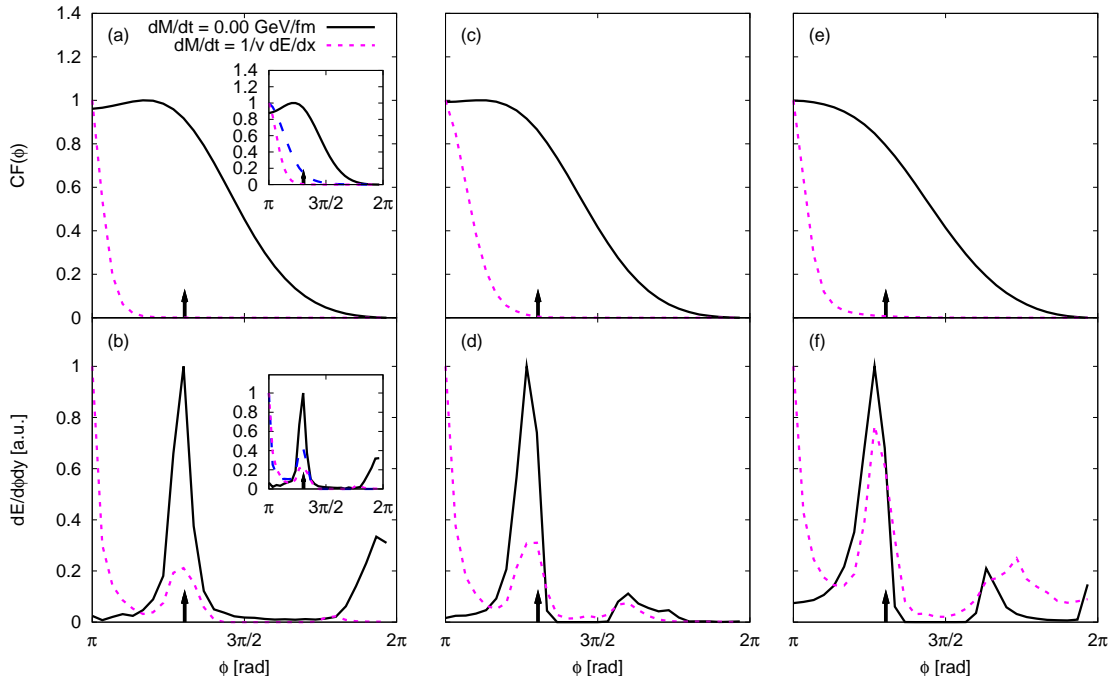


FIG. 6: (Color online) The normalized angular distribution generated by a decelerating jet (cf. also Fig. 5) at mid-rapidity is shown (upper panel) according to an isochronous Cooper–Frye freeze-out at  $p_{\perp} = 5$  GeV for a jet that stops after  $\Delta x = 4.5$  fm and a hydrodynamical evolution of  $t = 4.5$  fm (left panel),  $t = 6.5$  fm (middle panel) and  $t = 8.5$  fm (right panel). The corresponding bulk flow pattern [52] is shown in the lower panel. The solid black line in all plots depicts the pure energy deposition case while the dashed magenta line corresponds to the energy and momentum deposition scenario given by Eq. (12). The arrows indicate the angle of the Mach cone as computed via Mach’s law. The inserts repeat Fig. 2 (a) and (b) for comparison.

## V. SUMMARY

In this paper we compared the away-side angular correlations at mid-rapidity associated with uniformly moving jets and also decelerating jets in a static medium. In general, a fast moving parton will lose a certain amount of its energy and momentum along its path through the medium and thus decelerate. Therefore, depending on its energy the jet will either punch through the medium and fragment in the vacuum or it will be severely quenched until it cannot be distinguished from the other thermal partons in the plasma.

Our results confirm previous studies [23, 26, 33] where a similar source term [see Eq. (7)] was used to show that the diffusion wake created by these jets leads to a single peak in the away-side of the associated di-hadron correlations that overwhelms the weak Mach signal after isochronous CF freeze-out unless the total amount of momentum loss experienced by the jet is much smaller than the corresponding energy loss. However, according to the bulk energy flow the peak always occurs at the expected Mach cone angle but the diffusion wake still leads to a large peak in the associated jet direction when  $dM/dt \neq 0$  (see Fig. 2).

The same features also appear when different jet velocities are considered. In the bulk energy flow distribution the peaks occur nearly at about the expected Mach cone angles (for slow velocities they are shifted due to the creation of a bow shock), but in the CF freeze-out distribution these peaks only occur at large jet velocities (see Fig. 2). This result is consistent with the angular correlations obtained for a punch-through heavy quark jet [52] described by the Neufeld *et. al.* pQCD source term [53, 54, 55].

The diffusion wake created behind the jet dominates the freeze-out distribution for a jet moving through a static medium, even in case of large transverse momentum deposition (see Fig. 3) and independent of whether the jet has enough energy to punch through (see Fig. 1) the medium or not (Fig. 5). Assuming that the jet decelerates according to the Bethe–Bloch formalism, see Eq. (10), we checked whether the large amount of energy deposited around the stopping point (the well-known Bragg peak) can block the diffusion wake and thus alter the angular correlations. However, our results show that no significant differences occur between the away-side angular correlations associated with punch-through jets and decelerating jets described within the Bethe–Bloch model

(compare Fig. 2 and Fig. 6). Clearly, it would be interesting to study other models that describe decelerating jets in strongly-coupled plasmas. However, the simple Bethe–Bloch model used here displays the main qualitative features relevant for the hydrodynamic wake associated with decelerating jets. The path lengths of both types of jets were taken to be the same. A different scenario in which the light jets are almost immediately stopped in the medium while the heavy quark jets are still able to punch through may lead to different angular correlations. Such an analysis is left for a future study.

We would like to underline that the formation of a diffusion wake that trails the supersonic jet is a generic phenomenon [36] and, thus, its phenomenological consequences must be investigated and not simply neglected. Our results indicate that the diffusion wake is universal to all scenarios where momentum as well as energy is deposited to the medium, independent of whether the jet stops or is quenched. However, one can expect that the strong forward moving column of fluid represented by the diffusion wake can be considerably distorted in an expanding medium by the presence of a large radial flow. The interplay between radial flow and away-side

conical correlations in an expanding three-dimensional ideal fluid with a realistic equation of state [73] compatible with current lattice results [74] is currently under investigation.

### Acknowledgments

The authors thank I. Pshenichnov, L. Satarov, M. Bleicher, C. Greiner, P. Rau, J. Reinhardt, J. Steinheimer and H. Stöcker for helpful discussions and D. Dietrich for carefully reading the manuscript. The work of B.B. is supported by BMBF and by the Helmholtz Research School H-QM. J.N. and M.G. acknowledge support from DOE under Grant No. DE-FG02-93ER40764. M.G. also acknowledges sabbatical support from DFG, ITP, and FIAS at Goethe University. G.T. is grateful to LOEWE for the financial support given and thanks the Alexander von Humboldt foundation as well as Goethe University for support. I.M. acknowledges support from the grant NS-3004.2008.2 (Russia).

- 
- [1] K. Adcox *et al.* [PHENIX Collaboration], Phys. Rev. Lett. **88**, 022301 (2002).
  - [2] C. Adler *et al.* [STAR Collaboration], Phys. Rev. Lett. **90**, 082302 (2003).
  - [3] M. Gyulassy and M. Plumer, Phys. Lett. B **243**, 432 (1990).
  - [4] M. Gyulassy and X. n. Wang, Nucl. Phys. B **420**, 583 (1994).
  - [5] X. N. Wang, M. Gyulassy and M. Plumer, Phys. Rev. D **51**, 3436 (1995).
  - [6] R. Baier, Y. L. Dokshitzer, A. H. Mueller, S. Peigne and D. Schiff, Nucl. Phys. B **483**, 291 (1997).
  - [7] U. A. Wiedemann, Nucl. Phys. B **588**, 303 (2000).
  - [8] M. Gyulassy, P. Levai and I. Vitev, Nucl. Phys. B **571**, 197 (2000); Phys. Rev. Lett. **85**, 5535 (2000); Nucl. Phys. B **594**, 371 (2001); Phys. Rev. Lett. **86**, 2537 (2001); I. Vitev and M. Gyulassy, Phys. Rev. Lett. **89**, 252301 (2002).
  - [9] X. N. Wang and X. f. Guo, Nucl. Phys. A **696**, 788 (2001).
  - [10] P. Arnold, G. D. Moore and L. G. Yaffe, JHEP **0112**, 009 (2001); JHEP **0206**, 030 (2002).
  - [11] H. Liu, K. Rajagopal and U. A. Wiedemann, Phys. Rev. Lett. **97**, 182301 (2006).
  - [12] A. Majumder, B. Muller and X. N. Wang, Phys. Rev. Lett. **99**, 192301 (2007).
  - [13] J. Adams *et al.* [STAR Collaboration], Phys. Rev. Lett. **91**, 072304 (2003).
  - [14] S. S. Adler *et al.* [PHENIX Collaboration], Phys. Rev. Lett. **97**, 052301 (2006).
  - [15] J. Adams *et al.* [STAR Collaboration], Phys. Rev. Lett. **95**, 152301 (2005).
  - [16] J. G. Ulery [STAR Collaboration], Nucl. Phys. A **774**, 581 (2006).
  - [17] A. Adare *et al.* [PHENIX Collaboration], Phys. Rev. C **78**, 014901 (2008).
  - [18] B. I. Abelev *et al.* [STAR Collaboration], arXiv:0805.0622 [nucl-ex].
  - [19] P. F. Kolb and U. W. Heinz, arXiv:nucl-th/0305084.
  - [20] P. Romatschke and U. Romatschke, Phys. Rev. Lett. **99**, 172301 (2007).
  - [21] H. G. Baumgardt *et al.*, Z. Phys. A **273**, 359 (1975).
  - [22] J. Hofmann, H. Stoecker, U. W. Heinz, W. Scheid and W. Greiner, Phys. Rev. Lett. **36**, 88 (1976).
  - [23] J. Casalderrey-Solana, E. V. Shuryak and D. Teaney, J. Phys. Conf. Ser. **27**, 22 (2005) [Nucl. Phys. A **774**, 577 (2006)].
  - [24] H. Stoecker, Nucl. Phys. A **750**, 121 (2005).
  - [25] L. M. Satarov, H. Stoecker and I. N. Mishustin, Phys. Lett. B **627**, 64 (2005).
  - [26] J. Casalderrey-Solana, E. V. Shuryak and D. Teaney, arXiv:hep-ph/0602183.
  - [27] M. Gyulassy and L. McLerran, Nucl. Phys. A **750**, 30 (2005).
  - [28] E. V. Shuryak, Nucl. Phys. A **750**, 64 (2005).
  - [29] J. Casalderrey-Solana and E. V. Shuryak, arXiv:hep-ph/0511263.
  - [30] A. K. Chaudhuri and U. Heinz, Phys. Rev. Lett. **97**, 062301 (2006).
  - [31] T. Renk, J. Ruppert, C. Nonaka and S. A. Bass, Phys. Rev. C **75**, 031902 (2007).
  - [32] T. Renk and J. Ruppert, Phys. Rev. C **76**, 014908 (2007).
  - [33] B. Betz, M. Gyulassy, D. H. Rischke, H. Stocker and G. Torrieri, J. Phys. G **35**, 104106 (2008).
  - [34] S. A. Bass, C. Gale, A. Majumder, C. Nonaka, G. Y. Qin, T. Renk and J. Ruppert, arXiv:0808.0908 [nucl-th].
  - [35] B. Schenke, M. Strickland, A. Dumitru, Y. Nara and C. Greiner, arXiv:0810.1314 [hep-ph].



- [36] L. D. Landau and E. M. Lifshitz, *Fluid Mechanics*, (Pergamon Press, New York, 1987), Vol. 6.
- [37] P. M. Chesler and L. G. Yaffe, *Phys. Rev. Lett.* **99**, 152001 (2007).
- [38] S. S. Gubser, S. S. Pufu and A. Yarom, *Phys. Rev. Lett.* **100**, 012301 (2008).
- [39] A. Karch and E. Katz, *JHEP* **0206**, 043 (2002).
- [40] C. P. Herzog, A. Karch, P. Kovtun, C. Kozcaz and L. G. Yaffe, *JHEP* **0607**, 013 (2006).
- [41] S. S. Gubser, *Phys. Rev. D* **74**, 126005 (2006).
- [42] J. J. Friess, S. S. Gubser, G. Michalogiorgakis and S. S. Pufu, *Phys. Rev. D* **75**, 106003 (2007).
- [43] S. S. Gubser and A. Yarom, *Phys. Rev. D* **77**, 066007 (2008).
- [44] P. M. Chesler and L. G. Yaffe, *Phys. Rev. D* **78**, 045013 (2008).
- [45] J. Noronha, G. Torrieri and M. Gyulassy, *Phys. Rev. C* **78**, 024903 (2008); J. Noronha, M. Gyulassy and G. Torrieri, *J. Phys. G* **35**, 104061 (2008).
- [46] S. S. Gubser and A. Yarom, arXiv:0803.0081 [hep-th].
- [47] J. M. Maldacena, *Adv. Theor. Math. Phys.* **2**, 231 (1998) [*Int. J. Theor. Phys.* **38**, 1113 (1999)].
- [48] O. Aharony, S. S. Gubser, J. M. Maldacena, H. Ooguri and Y. Oz, *Phys. Rept.* **323**, 183 (2000).
- [49] J. Noronha and M. Gyulassy, arXiv:0806.4374 [hep-ph].
- [50] J. Noronha, M. Gyulassy and G. Torrieri, arXiv:0807.1038 [hep-ph].
- [51] M. Gyulassy, J. Noronha and G. Torrieri, arXiv:0807.2235 [hep-ph].
- [52] B. Betz, M. Gyulassy, J. Noronha and G. Torrieri, arXiv:0807.4526 [hep-ph].
- [53] R. B. Neufeld, B. Muller and J. Ruppert, *Phys. Rev. C* **78**, 041901 (2008).
- [54] R. B. Neufeld, *Phys. Rev. D* **78**, 085015 (2008).
- [55] R. B. Neufeld, arXiv:0807.2996 [nucl-th].
- [56] D. H. Rischke, Y. Pursun, J. A. Maruhn, H. Stoecker and W. Greiner, *Heavy Ion Phys.* **1**, 309 (1995).
- [57] F. Cooper and G. Frye, *Phys. Rev. D* **10**, 186 (1974).
- [58] H. Bethe, *Annalen der Physik* **397**, 325 (1930).
- [59] W. H. Bragg and R. Kleemann, *Philos. Mag.* **10**, 318 (1905).
- [60] G. T. Y. Chen, J. R. Castro and J. M. Quivey, *Ann. Rev. Biohys. Bioeng.* **10**, 499 (1981).
- [61] L. Sihver, D. Schardt and T. Kanai, *Jpn. J. Med. Phys.* **18**, 1 (1998).
- [62] U. Amaldi and G. Kraft, *Rep. Prog. Phys.* **68**, 1861 (2005).
- [63] R. R. Wilson, *Phys. Rev.* **71**, 385 (1947).
- [64] H. Eickhoff et. al., *The proposed accelerator facility for light ion cancer therapy in Heidelberg*, prepared for IEEE Particle Accelerator Conference (PAC 99), New York, New York, 29 Mar - 2 Apr 1999.
- [65] I. Pshenichnov, I. Mishustin and W. Greiner, *Phys. Med. and Biol.* **50**, 5493 (2005); **51**, 6099 (2006); I. Pshenichnov, A. Larionov, I. Mishustin and W. Greiner, *Phys. Med. and Biol.* **52**, 7295 (2007); I. Pshenichnov, I. Mishustin and W. Greiner, *Nucl. Inst. Meth.* **B 226**, 1094 (2008); O. I. Obolensky, E. Surdutovich, I. Pshenichnov, I. Mishustin, A. V. Solov'yov and W. Greiner, *Nucl. Inst. Meth.* **B 266**, 1623 (2008).
- [66] L. P. Csernai, *Introduction To Relativistic Heavy Ion Collisions*, John Wiley & Sons Ltd, Chichester, 1994.
- [67] R. J. Fries, B. Muller, C. Nonaka and S. A. Bass, *Phys. Rev. Lett.* **90**, 202303 (2003).
- [68] R. J. Fries, B. Muller, C. Nonaka and S. A. Bass, *Phys. Rev. C* **68**, 044902 (2003).
- [69] R. J. Fries, S. A. Bass and B. Muller, *Phys. Rev. Lett.* **94**, 122301 (2005).
- [70] V. Greco, C. M. Ko and P. Levai, *Phys. Rev. Lett.* **90**, 202302 (2003).
- [71] V. Greco, C. M. Ko and P. Levai, *Phys. Rev. C* **68**, 034904 (2003).
- [72] B. Betz, M. Gyulassy and G. Torrieri, *Phys. Rev. C* **76**, 044901 (2007).
- [73] J. Noronha-Hostler, J. Noronha and C. Greiner, arXiv:0811.1571 [nucl-th].
- [74] M. Cheng *et al.*, *Phys. Rev. D* **77**, 014511 (2008).